Canopy and reproductive development in mungbean (Vigna radiata)

Authors: Geetika, Geetika, Collins, Marisa, Singh, Vijaya, Hammer, Graeme, Mellor, Vincent, et al.

Source: Crop and Pasture Science, 73(10) : 1142-1155

Published By: CSIRO Publishing

URL: https://doi.org/10.1071/CP21209

RESEARCH PAPER
https://doi.org/10.1071/CP21209

CROP & PASTURE SCIENCE

Canopy and reproductive development in mungbean (*Vigna radiata*)

Geetika Geetika[A,*], Marisa Collins[B], Vijaya Singh[C], Graeme Hammer[C], Vincent Mellor[D], Millicent Smith[A,D] and Rao C. N. Rachaputi[A]

For full list of author affiliations and declarations see end of paper

***Correspondence to:**
Geetika Geetika
Queensland Alliance for Agriculture and Food Innovation, The University of Queensland, Gatton, Qld 4343, Australia
Email: geetika.geetika@uq.net.edu.au

Handling Editor:
Matthew Denton

ABSTRACT

Context. Mungbean (*Vigna radiata* (L.) Wilczek) is an important grain legume for food, feed, and green manure. Mungbean yield is highly variable due to fluctuating temperature and unpredictable rainfall. **Aims.** To improve yield stability, it is critical to utilise a model that can simulate mungbean phenology, biomass, and yield accurately. **Methods.** A thorough understanding of the physiological determinants of growth and yield is required to advance existing mungbean crop modelling capability. Currently, there is limited understanding of the physiological determinants of canopy and reproductive development and their variation in mungbean germplasm. Two experiments (controlled and field environments) were conducted at Gatton, Queensland, in 2018–19. Six Australian mungbean genotypes and one black gram (*Vigna mungo* L.) were grown under non-limiting conditions. Plant phenotypic traits (canopy development, time to first, 50% flowering, duration of flowering and podding, flower appearance, pod addition rates) were recorded. **Key results.** Genotypes M10403 and Satin II had significantly higher leaf appearance rate (LAR). Genotypes with a greater LAR had higher number of leaves but lower individual leaf area. Genotypes varied significantly in time to first and 50% flowering, with Onyx-AU (black gram) and Celera II-AU flowering earliest. Flowering and podding rates, and duration of these phenological phases varied among genotypes. Total plant leaf area (TPLA) approached its maximum at mid-podding stage. **Implications.** This study quantified the key phenotypic and physiological relationships associated with canopy and reproductive development, critical for the improvement of mungbean crop modelling required to accurately simulate growth and development and inform possible canopy constraints that are limiting mungbean productivity.

Keywords: black gram, flower appearance rate, green gram, leaf area development, pod addition rate, reproductive duration, source-sink dynamics, thermal time.

Received: 21 March 2021
Accepted: 22 March 2022
Published: 10 June 2022

Cite this:
Geetika G *et al.* (2022)
Crop & Pasture Science, **73**(10), 1142–1155.
doi:10.1071/CP21209

Introduction

Mungbean (*Vigna radiata* (L.) Wilczek) is a short-season legume, grown in sub-tropical regions globally. Mungbean seed is highly valued as a source of vegetable protein (~23% protein) (Akpapunam 1996) and is a staple food legume, particularly in Asia. India is the largest producer of mungbean, with the crop being cultivated on 3 million ha, followed by China and Myanmar (~0.6 and 0.7 million ha, respectively) (Nair *et al.* 2014).

Mungbean is produced in the summer-dominant rainfall areas of Australia and 95% of Australian grown mungbean is exported to Asian and American markets (Nair *et al.* 2013). Average yield for Australian mungbean over the last decade has been stagnant at 1.1 tonne ha^{-1} (Rachaputi *et al.* 2015), with a potential to attain over 2 tonnes ha^{-1} (Thomas *et al.* 2004; Chauhan and Williams 2018). Despite this, mungbean is generally regarded as a high-risk crop due to high yield variability (Chauhan and Williams 2018). Variability in yield is associated with several environmental and management factors, such as drought stress (Muchow 1985; Chauhan and Rachaputi 2014), heat stress (Kaur *et al.* 2015; Sharma *et al.* 2016), sowing time (Muchow *et al.* 1993) and row spacing (Rachaputi *et al.* 2019).

Approaches to improving yield and yield stability in mungbean can be informed by the use of crop models, which can simulate yield formation and adaptation in production systems (Robertson *et al.* 2015). For instance, using a simple crop model and participatory research approach with growers, Robertson *et al.* (2000) quantified the potential yield and price benefits of a spring sowing of mungbean and identified crop water supply as the predominant driver of yield variation in northern NSW and southern Qld.

Canopy development and reproductive dynamics drive yield formation and are key components of robust crop models for mungbean (Chauhan and Williams 2018). These traits have not been quantified for the current commercial Australian mungbean genotypes. This inhibits the development of robust crop models, that could contribute to improvements in agronomic management decisions in target production environments, where potential increases in yield and yield stability can be realised. Hence, a clear understanding and quantification of the traits that determine canopy and reproductive development is essential.

Canopy development is a key process that underpins radiation interception and water use by the crop. At the plant level, canopy development is determined by total number of leaves, leaf appearance rate (LAR) and leaf area, which combined, results in total plant leaf area (TPLA). Currently there is little information on contributions of these components to canopy development in mungbean. In their detailed review, Chauhan and Williams (2018) identified genetic variation in canopy development as a potential area to investigate for yield advance. Genotypic variation in leaf size has been reported in pigeonpea (*Cajanus cajan* (L.) Millsp.) (Ranganathan *et al.* 2001) and cowpea (*Vigna unguiculata* L.) (Littleton *et al.* 1979), whereby the size of newly expanded leaves increased with ontogeny, until individual leaf area reached a maximum, after which the size of new emerging leaves declined. Similarly, LAR, defined as the rate of appearance of leaves on the main stem per unit thermal time and the total number of leaves, is known to vary across crops such as rapeseed (*Brassica napus* L.) (Morrison and McVetty 1991), legumes (*Macroptilum lathyroides* L., *Vigna trilobata* L., *Sesbania* spp.) (Pengelly *et al.* 1999), and chickpea (*Cicer arietinum* L.) (Soltani *et al.* 2006). In mungbean, Robertson *et al.* (2002) found that cv. King required 100 degree-day for appearance of each leaf bearing node, while pigeonpea required 24 degree-day for appearance of each node on the main stem (Ranganathan *et al.* 2001). Contrastingly, some studies on leaf appearance rate and canopy development in winter season legumes such as chickpea (*C. arietinum*), faba bean (*Vicia faba* L.), field pea (*Pisum sativum* L.) and narbon bean (*Vicia narbonensis* L.) indicated that leaf appearance did not influence the rate of canopy development (Mwanamwenge *et al.* 1997). Hence, to clarify the role and importance of aspects of canopy development in mungbean, and quantify environmental and genotypic responses, detailed information on the traits contributing to canopy development under non-limiting conditions is required.

Canopy development is inherently coupled to phenology (Ravi Kumar *et al.* 2009), and both play a critical role in adaptation to abiotic stress. As the canopy develops, water demand increases, reducing the residual soil moisture during the reproductive phase, potentially impacting reproductive development if soil water is not replenished with irrigation or in-crop rainfall. The reproductive phase can be defined as the stage during which resources are directed more towards reproductive growth instead of vegetative organs such as stem and leaves (Cohen 1976). Floral development in mungbean can be related to both temperature and photoperiod (Chauhan and Williams 2018). Previous research on mungbean showed that in older Australian varieties, commencement of flowering was sensitive to photoperiod during the pre-anthesis stage (Imrie and Lawn 1990). However, photoperiod sensitivity of current varieties has not been characterised.

While the use of the current Agricultural Production Systems sIMulator (APSIM) mungbean crop model has provided hypotheses about avenues to improve adaptation in mungbean (Chauhan and Williams 2018), improved understanding and quantification of canopy development and reproductive dynamics for relevant germplasm is required to progress. The broad intent of this study is to generate a firm biophysical basis to enhance existing modelling capability so that robust and credible simulation studies on appropriate genetic and agronomic manipulations targeting yield improvement in mungbean can be pursued. Specifically, this study aims to close the knowledge gaps and generate quantitative relationships on canopy development and reproductive dynamics in mungbean by quantifying: (1) variation in canopy development dynamics in key Australian mungbean genotypes, by assessing leaf appearance rate (LAR), main stem node number (MSNN), leaf size, and their relationship with total plant leaf area (TPLA); and (2) genotypic variation in reproductive phenology by investigating the dynamics of flower and pod addition, and its effects on TPLA.

Materials and methods

Plant material

Two experiments were undertaken at The University of Queensland that included six mungbean (*Vigna radiata* L.) and one black gram (*Vigna mungo* L.) genotypes (see Supplementary materials Table S1). These genotypes were produced and commercialised by the National Mungbean Improvement Program, Queensland Department of Agriculture and Fisheries (DAF). Mungbean genotypes Jade-AU, Berken, Satin II and Opal-AU have medium to large seeds, with Celera II-AU and M10403 having small seeds. Black gram is closely related, though biologically distinct, from mungbean. Black gram, Onyx-AU was included in this study to quantify

its canopy development, branching pattern and reproductive development in relation to mungbean. Onyx-AU has black seeds and superior halo blight resistance in comparison to mungbean genotypes (Table S1).

Experiment details

The two experiments were conducted during the summer growing season of 2018–19 at the University of Queensland, Gatton campus (27°33′S, 152°20′E) in south-east Queensland, Australia, one in the controlled environment glasshouse (GH Expt) and the other in the field (FLD Expt).

Controlled environment experiment (GH Expt)

The genotypes were sown in 4-L pots in controlled environment glasshouse on 16 December 2018. The pots were placed on steel mesh benches in a randomised block design, with three replications. Before sowing, pots of 4-L capacity (ANOVApot, 200 mm diameter) were filled with a black vertosol soil collected from Dalby in south-east Queensland (Queensland Government 2016). Before filling, the soil was spread, fan-dried and lumps broken down. Fertiliser was added to the dried soil by mixing 32 L of soil with 8 g of Granulock Z (Incitec Pivot Fertilisers) compound fertiliser (11% N, 21.8% P, 4% S, 1% Zn), added at a rate of 40 kg ha^{-1} of nitrogen in a cement mixer until the mixture was homogenous. Each pot was filled to a weight of 4 kg of dry soil. All pots were hand-watered and allowed to drain overnight. Each steel bench was of 0.8 m width and 2.4 m length and accommodated a total of 24 pots, with ~20 cm spacing between any two respective pots. The benches were placed away from the walls to ensure light was not limiting.

Seeds were inoculated with Group I Inoculum (*Rhizobium* strain CB 1015) to ensure establishment of rhizobia in root nodules to promote atmospheric nitrogen fixation. Before sowing, seeds were treated with a fungicide, Thiram 600 (Group M3 fungicide) (Nufarm, Victoria, Australia). Four seeds were sown in the centre of each pot at a depth of 5 cm. Plants were watered daily via capillary matting attached to an automatic watering system. Emergence was defined as the stage when cotyledons and the hypocotyl were above the soil surface, showing epigeal emergence. Emerged seedlings were gradually thinned to one plant per pot by 15 days after sowing (DAS). Plants were watered daily to field capacity. SEASOL (seaweed solution) and PowerFeed (dynamic fertiliser and soil conditioner) (w/v 12% N, 1.4% P, 7% K) (Seasol International Pty Ltd, Victoria, Australia) were applied fortnightly, starting from 21 DAS, at a rate of 0.03 mL L^{-1} of water.

Growing environment. The ambient day/night temperatures in the glasshouse were set at 28°C/20°C, with the transition occurring daily at 6 am and 6 pm, respectively. Vapour pressure deficit (VPD) inside the glasshouse was 0.9 kPa. Temperature data was obtained at 10 min intervals from automatic temperature sensors located on the front wall inside the glasshouse

On average, the daily total solar radiation received by the plants was 17.5 MJ m^{-2} day^{-1} (~9 MJ m^{-2} day^{-1} of photosynthetically active radiation, PAR). Incident solar radiation was obtained from the Bureau of Meteorology (Australian Bureau of Metrology 2021) weather station located at the University of Queensland, Gatton campus (station number-040082). There was a 30% reduction in incident solar radiation inside the glasshouse, with this value being lower by ~12% around 1200 hours.

Measurements. *Canopy development*: The number of nodes, leaves (both apical and expanded leaves) and branches were counted as they appeared on main stem and branches in all replications every other day. A node was recorded as fully developed when its associated leaf was fully unfolded and flat. Counting nodes began at the base of the stem with two-leaf unifoliate node being counted as node number one.

Leaf appearance rate (LAR), defined as the proportion of leaf emerged per unit of thermal time, was calculated as the total number of leaves on the main stem divided by the cumulative thermal time from 1 DAS (Morrison and McVetty 1991). A leaf was considered as appeared once the leaflet was fully emerged from the leaf primordia.

Total plant leaf area (TPLA) was estimated for all genotypes in the GH Expt. Leaf area (size) of trifoliate and unifoliate leaves at each node on the stem was measured at the final harvest, using a LICOR planimeter (LI-3000), with an accuracy of ±2%. TPLA ($plant^{-1}$) was computed by summing up the individual leaf size at each node on the plant. Average leaf area ($plant^{-1}$) was calculated as a ratio between TPLA and total number of leaves.

Reproductive development: Time to first flower was scored when 50% of the plants for each genotype had at least one flower open. Time to 50% flowering was estimated when 50% of total flowers had opened for each genotype. The number of opened flowers and visible immature pods were counted on alternate days and the cumulative open flower number and immature pod number per genotype was calculated.

Field experiment (FLD Expt)

The second experiment was conducted in the field at the University of Queensland, Gatton campus, Gilbert paddock (27°56′S, 152°33′E). The experimental block was fallow for 6 months after a sorghum (*Sorghum bicolor* L.) crop and was prepared by power harrowing. The experiment was sown on 8 February 2019. Five of the six genotypes of mungbean (M10403 was omitted due to lack of seed availability) and Onyx-AU were planted. Seeds were inoculated with Group I Inoculum (*Rhizobium* strain CB 1015) to ensure establishment of rhizobia in root nodules to promote nitrogen fixation. The experiment was set-up as

a randomised block design with four replications, with each plot being 3.6 m wide and 5 m long, with inter-row spacing of 0.4 m and density of 38 plants m^{-2}. Pre-sowing soil analysis indicated sufficient soil nitrogen however, a 25 kg ha^{-1} of Granulock Z (N:11%, P:21.8%, S:4%, Zn:1%) was applied as part of a standard practise to ensure nutrients were not limiting. After sowing, a pre-emergent herbicide, Dual Gold (Syngenta, Australia) (2 L ha^{-1}) was applied at a target rate of 150 L ha^{-1} to manage weeds. 95% emergence was noted after 6 DAS. The trial received optimal irrigation, with no apparent water deficit. The field trial was managed with weeding and insecticides and fungicides were applied as required. An Altacor (active 350 g kg^{-1} Chlorantraniliprole) spray, at a rate of 70 g ha^{-1} for *Helicoverpa* control was done. This was followed by a spray of Dimethoate salt at 500 mL ha^{-1}. Three applications of Sumi-AlfaFlex (active 50 g L^{-1} Esfenvalerate) at a rate of 500 mL ha^{-1} were completed at different times over the growing season to control a broad range of insects.

Growing environment. The crop received an average of 17.1 MJ m^{-2} day^{-1} of solar radiation (~9 MJ m^{-2} day^{-1} of PAR), with average daily maximum and minimum temperatures of 30°C and 15°C, respectively. On average, VPD in the field was about 20% higher in comparison to the GH Expt (i.e. 1.0 kPa). The crop received a total of 128 mm of rainfall and 90 mm of irrigation, which was sufficient to avoid water limitation throughout the crop life cycle.

Data for daily temperature, solar radiation and relative humidity were obtained from a remote monitoring sensor station (RX3000 HOBO Data Loggers, Australia), located 100 m from the experiment site, with data recorded at an interval of 5 min. Rainfall data was obtained from the Bureau of Metrology (BOM, Australia) station for Gatton (station number-040082).

Measurements. Observations for canopy development and phenology were undertaken following protocol as described for GH Expt.

Thermal time (TT) calculation: For both the controlled environment and field experiments, thermal time for each day (TT_i) was calculated from a piecewise linear function of temperature (T) (Eqn 1):

$$TT_i = \begin{cases} T_b - T & T_b < T < T_{opt} \\ (T_{opt} - T_b)\left[1 - \frac{T - T_{opt}}{T_{max} - T_{opt}}\right] & \text{where } T_{opt} < T < T_{max} \\ 0 & \text{Otherwise} \end{cases} \quad (1)$$

where T_b was base temperature, T_{opt} was optimum temperature, and T_{max} was maximum temperature, with values of 7.5°C, 30°C and 40°C, respectively (Ellis *et al.* 1994; Chauhan and Williams 2018).

To minimise error associated with diurnal temperature range, the daily calculation was derived from eight 3-hourly calculations as described by Jones and Kiniry (1986) and Hammer *et al.* (1993). TT_i to the end of any specific phase was determined by accumulating TT_i from 1 DAS until the final day of each phase.

Quantification of total plant node number (TNN): In the GH Expt, the relationship between total plant node number (TNN) and main stem node number (MSNN) was quantified by fitting a bi-linear model, as described by Soltani *et al.* (2006), which separates node production into different phases; *Phase I* is when TNN increases at a slower rate and *Phase II* has a higher rate of node production and can be described as follows:

$$TNN = \begin{cases} a_{1x} & \text{if } x \le x_0 \quad \text{(Phase I)} \\ a_{1x} + a_2(x - x_0) & \text{if } x > x_0 \quad \text{(Phase II)} \end{cases} \quad (2)$$

where x is the number of nodes on main stem, x_0 is the turning point between the two phases of node production, a_1 the rate of increase in total node number in *Phase I* and a_2 the same as a_1 for *Phase II* of node production. It should be noted that the main stem individual nodes may also have a secondary node, which is counted in the total plant node number (TNN).

Computing total plant leaf area (TPLA): A logistic function was used as a descriptor of total plant leaf area (TPLA) based on thermal time in R studio, using nlsList (Pinheiro *et al.* 2021) for GH Expt:

$$TPLA = \frac{TPLA_{max}}{1 + e^{-k(a - TT)}} \quad (3)$$

where $TPLA_{max}$ is the maximum TPLA attained, a (x-mid) refers to the thermal time required for TPLA to reach half of $TPLA_{max}$, and k is a curvature coefficient, which was common across genotypes.

Estimation of flower and pod addition rates: For both the controlled glass house and field experiments, cumulative flower and pod numbers were quantified by fitting a three-parameter sigmoid function on thermal time (x) in R studio, using SSlogis function, which has been widely used for crop growth modelling (Overman and Scholtz 2002):

$$\text{Cumulative flower/pod number} = \frac{Asym}{1 + \exp\left(\frac{x_{mid} - x}{k}\right)} \quad (4)$$

where Asym is the upper asymptote (potential flower/pod number), x_{mid} is the inflexion point (degree-day), and k is a curvature coefficient. x_{mid} was used to determine the duration of flowering and podding. The reciprocal of

the k value (degree-day Flower^{-1} and degree-day pod^{-1}) estimated from Eqn 4 was taken to calculate the flower appearance rate (flower (degree-day)$^{-1}$) and pod addition rate (pod (degree-day)$^{-1}$) for each genotype.

Statistical analysis

Linear mixed model (LMM) analyses were performed in R software (R Core Team 2021) using the nonlinear mixed-effects (NLME) algorithm (Pinheiro *et al.* 2021) and the emmeans package (Lenth 2021) for LAR. Slopes for LAR for the genotypes were compared using lstrends (used for estimating and comparing the slopes of fitted lines) and Tukey HSD with the significance level at $P < 0.05$. For linear regressions, Pearson's correlation coefficient test, which is a measure of strength of a linear association between two variables, was conducted to check for significance at $P < 0.05$. An analysis of co-variance (ANCOVA) was carried out to test for genotypic differences for TPLA, FAR and PAR using nlsList. Akaike information criterion (AIC) is a statistical measure for comparative evaluation among models, with the best model, which gives a good balance of goodness of fit and complexity, being the one with lowest AIC value (Profillidis and Botzoris 2019). Analysis of variance (ANOVA) was carried out to test for genotypic differences in main stem node number, total node number, total number of leaves, leaf area, total plant leaf area and LAR ($P < 0.05$) in Genstat 16th edition (Nelder 2017).

Results

Differences in temperatures between the GH Expt and FLD Expt resulted in differences in daily TT_i (Fig. 1). The cumulative thermal time to maturity observed in the two experiments was 1154 degree-day and 1030 degree-day for the glasshouse and field experiments, respectively.

Canopy development

Leaf appearance rate (LAR)

LAR (leaf (degree-day)$^{-1}$) was assessed in the GH Expt and FLD Expt. LAR can be regarded as a measure of node appearance rate. Genotypes differed significantly for LAR on the main stem ($P < 0.001$) in both experiments (Table 1), with the rates varying between 6 and 16% among mungbean genotypes in FLD Expt and GH Expt, respectively.

In the GH Expt, the LAR of Jade-AU and Opal-AU were similar, but the LAR of Jade-AU was significantly lower than Berken, Celera II-AU, M10403 and Satin II (Table 1). A similar result was observed in the field (FLD Expt), whereby Jade-AU had a similar LAR to Opal-AU which was also significantly lower in LAR [0.0130 Leaf (degree-day^{-1})] than Berken, Celera II-AU and Satin II [0.0139 Leaf (degree-day^{-1})]. LAR of the black gram (*V. mungo*) genotype, Onyx-AU was higher than all mungbean genotypes in GH Expt but similar to Jade-AU and Opal-AU in the field (Table 1). While the rankings of mungbean genotypes for LAR were similar across experiments, the magnitude differed with LAR being 23% greater on average in the FLD Expt.

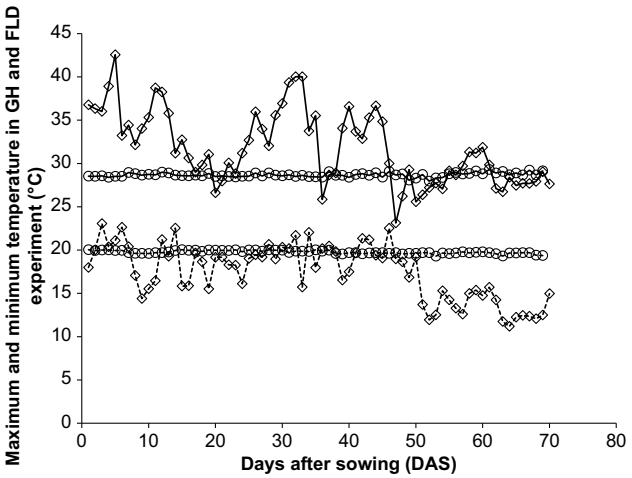

Fig. 1. Daily maximum (solid line) and minimum (dashed line) temperature in the glasshouse [GH (○)] and field [FLD (◇)] experiments versus days after sowing (DAS).

Table 1. Mean leaf appearance rate (LAR) on the main stem for genotypes in the glasshouse (GH) and field (FLD) experiments.

Genotype	LAR (leaf (degree-day)$^{-1}$) (GH Expt)	LAR (leaf (degree-day)$^{-1}$) (FLD Expt)
Jade-AU	0.0096a	0.0130a
Opal-AU	0.0099ab	0.0130a
Berken	0.0101b	0.0138b
Celera II-AU	0.0104b	0.0138b
M10403	0.0111c	NT
Satin II	0.0111c	0.0139b
Onyx-AU	0.0127d	0.0131a

Letters denote significance between genotypes at $P < 0.05$.
NT, not tested.

Relationship between main stem node number (MSNN) and total node number (TNN)

Main stem node number differed significantly ($P < 0.001$) among genotypes in GH Expt ranging between seven and 12 nodes, with Onyx-AU having the highest MSNN (Table 2). TNN (plant^{-1}) varied significantly among the genotypes ($P < 0.001$), with M10403 and Onyx-AU having the highest TNN.

Table 2. Mean main stem node number, total node number, primary branch number, and total branch number at final harvest in the glasshouse (GH Expt) experiment.

GH Expt	Genotype						
	Berken	Jade-AU	Satin II	Opal-AU	M10403	Celera II-AU	Onyx-AU
Main stem node number	7.3a	7.3a	8.0a	8.3ab	10.3bc	8.3ab	11.7c
Total node number	11.0a	12.7a	12.7a	12.3a	21.0b	15.3ab	22.7b
Primary branch number	2.0a	3.0a	2.3a	2.3a	4.7a	4.3a	3.3a
Total branch number	3.7a	5.3ab	4.7ab	4.0a	10.7b	7.0ab	11.0b

Data are the means of three replications per genotype. Letters denote significance between genotypes at $P < 0.05$.

Total branch number differs but branching patterns are uniform

Primary branch number did not significantly differ between genotypes and on average all produced three primary branches (Table 2). However, there were significant differences ($P = 0.0042$) in total branch number between genotypes with Berken, Jade-AU, Satin II and Opal-AU producing 50% less total branches in comparison to Celera II-AU, M10403 and Onyx-AU. Celera II-AU had an intermediate branching tendency, with seven total branches, whereas M10403 and Onyx-AU produced the most branches (11 branches each). 58% of the primary branches originated from lower node numbers (1–3; unifoliate, Branch 1 and Branch 2), with the remainder originating from middle nodes (4, 5; Branch 3-Branch 4).

Despite differences in total branch number (Table 2), branching patterns over time for all genotypes were uniform (Fig. 2). The relationship between MSNN and TNN was quantified using a bi-linear model (Fig. 2). TNN accumulated a relatively lower rate of nodes in *Phase I* (rate = 1.05), followed by accelerated accumulation of node number in *Phase II*. For all genotypes, the higher rates of TNN accumulation were due to appearance of primary and secondary branches after an average of six nodes had developed on the main stem. The relationship fitted all mungbean genotypes as those with greater TNN had greater MSNN.

Genotypic variation in leaf size distribution

Individual leaf size showed a bell-shaped relationship with MSNN (Fig. 3). Individual leaf size (cm^2) at each node on the main stem differed significantly among genotypes in the GH Expt ($P < 0.001$) and differences in individual leaf size increased with each ascending node until maximum individual leaf size was attained. Maximum leaf size was attained at node number 6 for Opal-AU, Berken, Jade-AU, Celera II-AU, and Onyx-AU, while for Satin II, and M10403, individual leaf size on the main stem peaked at node 7 (Fig. 3). Opal-AU had the largest individual leaf size on the main stem, followed by M10403, Berken, Jade-AU, Satin II and Celera II-AU among mungbean genotypes. There was a decline in individual leaf size on the main stem after maximum leaf size was attained.

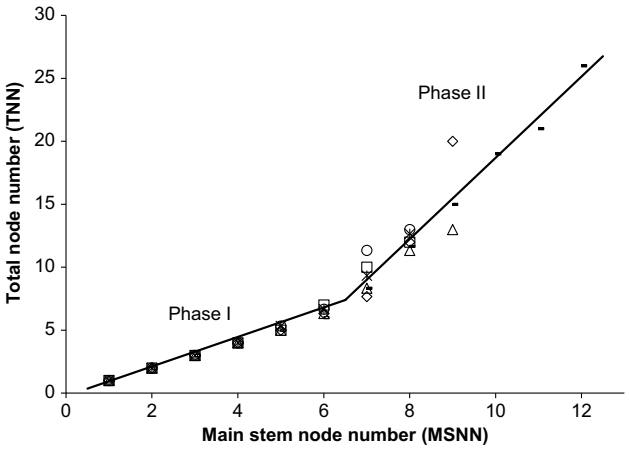

Fig. 2. Total plant node number (TNN) versus main stem node number (MSNN) for mungbean genotypes in the glasshouse experiment (GH Expt); Jade-AU (○), Celera II-AU (◇), Opal-AU (△), M10403 (-), Satin II (*) and Berken (□). Regression: Phase I: TNN = 1.05 × MSNN, (R^2 = 0.99) and Phase II: TNN = 3.25 × MSNN − 13.63 (R^2 = 0.94).

Leaf area production model

TPLA in the GH Expt (Fig. 2) was the product of the total number of nodes present and the size of individual leaves, with the total number of nodes being related to MSNN and hence to the rate of LAR. However, there was a significant negative correlation between LAR and average leaf size (Table 3) as explained by the following regression equation (data not shown):

$$\text{Average leaf size} = 236.41 - 12560 \times \text{LAR}, n = 19, R^2 = 0.26, P = 0.026 \quad (5)$$

This indicated that genotypes with slower LAR spent greater thermal time per leaf or node and had larger leaves and branched less (fewer TNN or total number of leaves) compared to genotypes with faster LAR, which branched more (higher TNN or total number of leaves) (Table 3). For example, across all genotypes, Onyx-AU had the highest LAR (0.0111) and total number of leaves (~23 leaves $plant^{-1}$), but smaller average leaf size (93 cm^{-2}), while Jade-AU had the lowest LAR (0.0079), 12 total leaves $plant^{-1}$

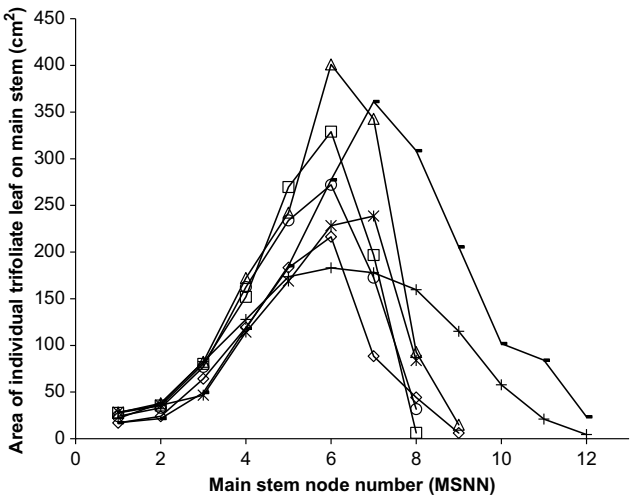

Fig. 3. Relationship between size of individual leaves (cm^2) on the main stem and main stem node number (MSNN) for Jade-AU (○), Opal-AU (△), Berken (□), Celera II-AU (◇), M10403 (-), Satin II (✳) and Onyx-AU (+) in glasshouse experiment (GH Expt). Each data point is an average across three replications.

and a leaf size of 126 cm^{-2} (Table 4). This also resulted in variations in TPLA (Table 3).

Relationship between TPLA and TT_i

The logistic equation fitted individual plant data well for all genotypes in the GH Expt (Fig. 4). Coefficients of the logistic function, $TPLA_{max}$ and *a* (thermal time required to reach half of $TPLA_{max}$) were significantly different among the genotypes. M10403 had the highest $TPLA_{max}$ and required the most thermal time to reach half $TPLA_{max}$ while Celera II-AU had the lowest $TPLA_{max}$ and required the smallest thermal time to reach half $TPLA_{max}$. $TPLA_{max}$ was influenced by TNN and leaf size, while *a*, which is the thermal time required to reach half $TPLA_{max}$, indicated the time after which plants began reductions in canopy expansion. Hence, TPLA in mungbean can be simulated if the two coefficients in Eqn 3, ($TPLA_{max}$ and *a*) are known or can be predicted.

Reproductive development

Genotypic variation in reproductive development

Genotypic differences between mungbean and black gram led to variation in flowering patterns. Flowering in mungbean (Fig. S1*a*) began on the uppermost nodes (e.g. node number 5) on the main stem first and then progressed to the lower nodes and branches, whereas, flowering in Onyx-AU started from lower nodes (e.g. node number 3) on the main stem and progressed upwards (Fig. S1*b*).

Genotypes differed significantly ($P < 0.001$) in the thermal time required to reach first flower in the GH Expt but not in the FLD Expt (Table 4). Similarly, time to 50% flowering was significantly different ($P < 0.001$) among genotypes in the GH Expt and the FLD Expt ($P = 0.008$). Generally, averaged across both experiments, there was a trend towards earlier first flowering in Onyx-AU and Celera II-AU compared to other genotypes. However, time to 50% flowering occurred much later in Onyx-AU (829.9 GDD) compared to mungbean genotypes, indicating a possible longer duration of flowering in Onyx-AU (865.4 GDD) (Table 4).

Appearance and duration of flowering and podding

The cumulative flower number could be quantified using a sigmoidal function on thermal time for all genotypes across the two experiments (Fig. 5). There was a strong genotypic effect for all the sigmoid coefficients describing the relationship between average cumulative number of flowers and thermal time. Onyx-AU produced significantly more flowers in both experiments. For the mungbean genotypes in the GH Expt, M10403 had the highest total flower number (65 flowers) but other genotypes were similar and on average produced 37 flowers $plant^{-1}$ (Fig. 5*a*, *c*). However, genotypes differed significantly ($P < 0.05$) in time taken to reach mid-flowering (*x*-mid), which is an

Table 3. Mean total number of leaves per plant, leaf appearance rate (LAR) on the main stem, average leaf size, and total plant leaf area for genotypes in the glasshouse experiment (GH Expt).

Genotype	Total number of leaves ($plant^{-1}$)	LAR on main stem [leaf (degree-day)$^{-1}$)]	Average leaf size (cm^2)	Total plant leaf area (cm^2 $plant^{-1}$)
Berken	11.0a	0.0087ab	144c	1572ab
Onyx-AU	22.7c	0.0111c	93ab	2105bc
Celera II-AU	15.3abc	0.0089ab	70a	1004a
Jade-AU	12.0ab	0.0079a	126bc	1496ab
M10403	21.0bc	0.0095abc	127bc	2678c
Opal-AU	12.3a	0.0084ab	151c	1867abc
Satin II	12.7a	0.0098bc	110abc	1396ab

The data excludes one plant for Jade-AU due to premature leaf shedding. Letters denote significance between genotypes at $P < 0.05$.

Table 4. Mean thermal time to first and 50% flower in six mungbean genotypes (Jade-AU, Opal-AU, Satin II, Celera II-AU, Berken and M10403) and black gram (Onyx-AU) in glasshouse (GH) and field (FLD) experiments.

Experiment	Genotype	Thermal time to first flower (degree-day)	Thermal time to 50% flower (degree-day)
Glasshouse (GH)	Onyx-AU	618c	847bc
	Celera II-AU	625bc	765d
	Berken	653bc	804cd
	Satin II	659bc	798cd
	Jade-AU	676b	856bc
	Opal-AU	678b	886b
	M10403	868a	997a
Field (FLD)	Celera II-AU	622a	740b
	Berken	624a	731b
	Satin II	626a	761b
	Jade-AU	628a	750b
	Opal-AU	628a	756b
	Onyx-AU	641a	813a

Each data point is an average across three and four replications in glasshouse (GH) and field (FLD) experiment, respectively. Letters denote significance between genotypes at $P < 0.05$.

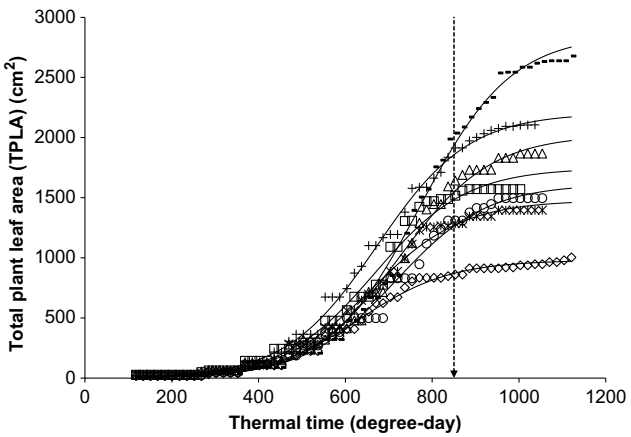

Fig. 4. Relationship between total plant leaf area (TPLA) (cm^2) and thermal time (degree-day) from sowing for Berken (□), Jade-AU (○), Celera II-AU (◇), M10403 (-), Opal-AU (△), Satin II (✳) and Onyx-AU (+) in the glasshouse experiment (GH Expt). Dashed vertical line indicates average mid-podding stage across genotypes. Data points are means across replications. Goodness of fit for each genotype is shown by the AIC values, with a low AIC indicating a better fit. The fitted values for each genotype were: TPLA – Berken: $y = 1745.7/(1 + \exp^{(-105.3 \times (667.7-X))})$, AIC = 613; Jade-AU: $y = 1612.4/(1 + \exp^{(-105.3 \times (715.1-X))})$, AIC = 622; Celera II-AU: $y = 979.8/(1 + \exp^{(-105.3 \times (632.2-X))})$, AIC = 566; M10403: $y = 2853.8/(1 + \exp^{(-105.3 \times (771.6-X))})$, AIC = 684; Opal-AU: $y = 2021.0/(1 + \exp^{(-105.3 \times (725.3-X))})$, AIC = 630; Satin II: $y = 1478.5/(1 + \exp^{(-105.3 \times (659.9-X))})$, AIC = 589; Onyx-AU: $y = 2202.3/(1 + \exp^{(-105.3 \times (673.0-X))})$, AIC = 591.

indicator of flowering duration. For example, Celera II-AU had the shortest flowering duration (mean of 749.7 degree-day across experiments). The genotypic differences were similar in the FLD Expt compared to the GH Expt, except for differences in total number of flowers and pods. Flower appearance rate (FAR) (flower (degree-day)$^{-1}$) varied significantly among genotypes (Table 5) in GH Expt, with Berken and Celera II-AU having the highest FAR among mungbean genotypes compared to Jade-AU (Table 5).

For PAR, a similar trend to flowering was noted and this was also quantified well via a sigmoidal growth curve (Fig. 5*b*, *d*). Any differences in pod addition reflected those found for FAR (Table 5). There was a high percentage of pod set with on average, 87% of flowers being converted into pods across the two experiments. PAR was significantly positively correlated with FAR, explained by the regression below (data not shown):

$$\text{PAR} = 0.0023 + (0.87 \times \text{FAR}),\ n = 13,\ R^2 = 0.87,\ P < 0.001 \quad (6)$$

The pod set data does not include pod abscission rates, which are generally higher in the field.

Interaction between TPLA and podding

The results in the present study indicated that there was a significant positive relationship between thermal time at onset of podding (initiation) and *a* (thermal time to reach half of $TPLA_{max}$) (Fig. 6*a*), likely due to plants transitioning from canopy development to reproductive development. However, this relationship became highly significant by mid-podding stage (Fig. 6*b*). Thermal time to mid total pod number varied among the genotypes and ranged between 755 and 980 degree-day. The positive relationship with thermal time to reach half of $TPLA_{max}$ indicated that the near cessation in growth of total plant leaf area (cm^2) was associated with the timing of rapid pod addition (Fig. 6*a*, *b*).

Discussion

Understanding and quantifying canopy development and reproductive dynamics is critical in underpinning the development of robust crop models for use in simulation studies of crop adaptation. Such adaptation analyses provide means to explore the influence of trait and management options on yield likelihood in target production environments. Canopy development is critical to establishing the dynamics of radiation capture and, hence, crop growth and potential water use. The interaction with phenology via crop duration and the timing of flower and pod addition influences the extent of canopy development and the likely incidence of terminal stress in water-limited environments.

Robust crop models can capture these dynamics once they are understood and quantified. For example, Robertson *et al.* (2000) demonstrated the potential of a

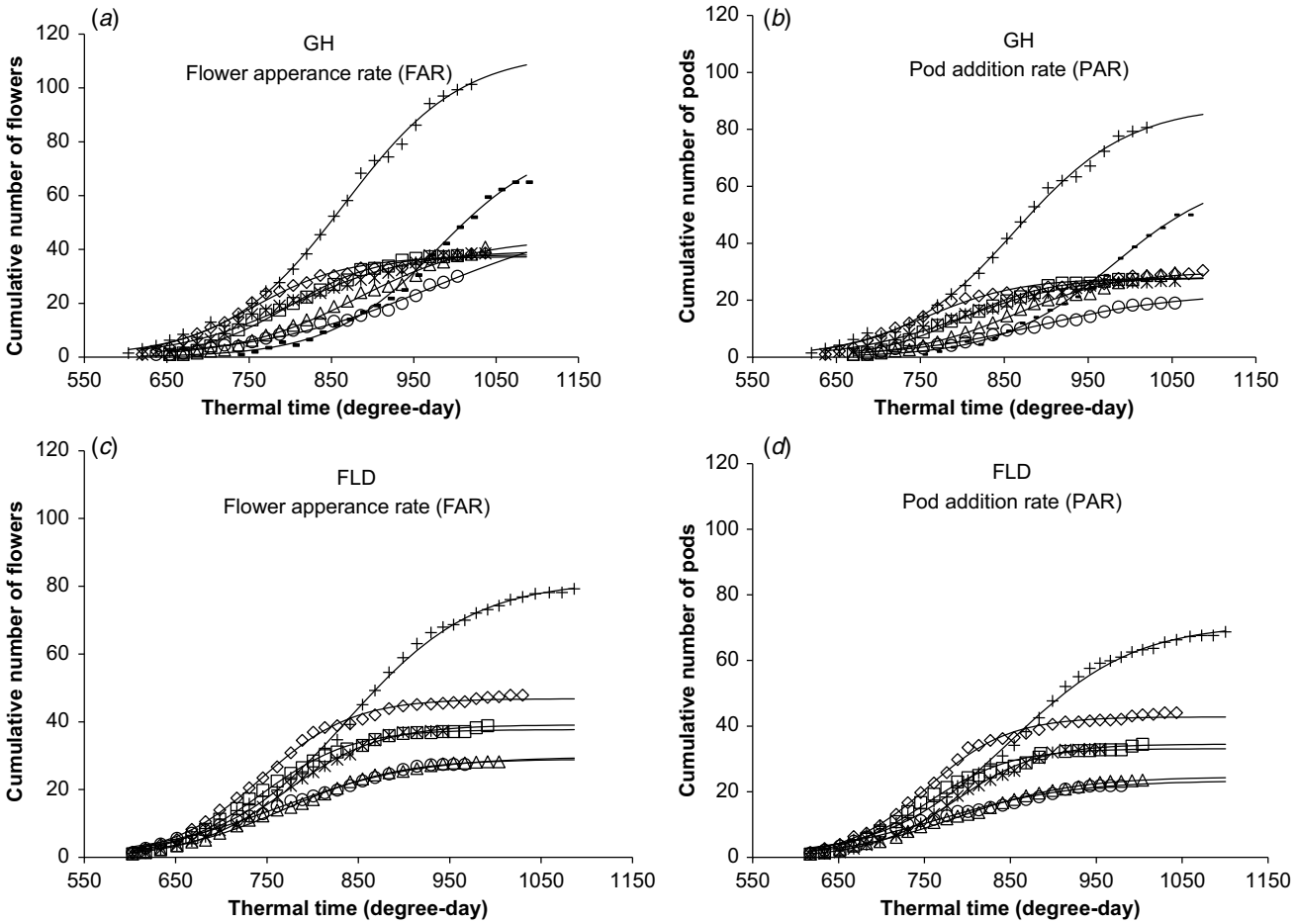

Fig. 5. Estimation of flower appearance rate (FAR) and pod addition rate (PAR) from cumulative flower and pod number as a function of thermal time (degree-day) for glasshouse (GH Expt) and field experiment (FLD Expt). Each data point is an average of cumulative flower and pod number across three pots in GH Expt and eight plants in FLD Expt. Genotypes are shown as Jade-AU (○), Opal-AU (△), M10403 (-), Celera II-AU (⋄), Berken (□), Onyx-AU (+), Satin II (✳) and Onyx (+). A common curve form (Eqn 4 – coefficients A_{sym}, x_{mid}, k) was fitted to all results. Goodness of fit for each genotype is shown by the AIC values, with a low AIC indicating a better fit. The fitted values for each genotype were: (*a*) GH Expt Flower number – Berken: $y = 38.1/(1 + \exp^{((798.6-X)/53.6)})$, AIC = 76; Jade-AU: $y = 52.4/(1 + \exp^{((974.9-X)/105.8)})$, AIC = 73; Celera II-AU: $y = 37.3/(1 + \exp^{((755.1-X)/57.1)})$, AIC = 110; M10403: $y = 81.0/(1 + \exp^{((979.7-X)/66.0)})$, AIC = 82; Opal-AU: $y = 44.1/(1 + \exp^{((882.2-X)/72.4)})$, AIC = 82; Satin II: $y = 39.6/(1 + \exp^{((804.0-X)/71.8)})$, AIC = 103; Onyx-AU: $y = 113.4/(1 + \exp^{((865.4-X)/71.3)})$, AIC = 105. (*b*) GH Expt Pod number – Berken: $y = 27.7/(1 + \exp^{((801.1-X)/50.5)})$, AIC = 53; Jade-AU: $y = 22.4/(1 + \exp^{((891.8-X)/83.3)})$, AIC = 45; Celera II-AU: $y = 27.8/(1 + \exp^{((754.8-X)/56.8)})$, AIC = 110; M10403: $y = 65.0/(1 + \exp^{((979.5-X)/67.4)})$, AIC = 64; Opal-AU: $y = 30.0/(1 + \exp^{((861.9-X)/62.5)})$, AIC = 63; Satin II: $y = 28.1/(1 + \exp^{((800.7-X)/66.3)})$, AIC = 64; Onyx-AU: $y = 88.4/(1 + \exp^{((862.5-X)/67.9)})$, AIC = 92. (*c*) FLD Expt Flower number – Berken: $y = 37.7/(1 + \exp^{((744.8-X)/48.5)})$, AIC = 69; Jade-AU: $y = 29.7/(1 + \exp^{((764.3-X)/75.5)})$, AIC = 56; Celera II-AU: $y = 46.8/(1 + \exp^{((744.2-X)/49.2)})$, AIC = 84; Opal-AU: $y = 29.0/(1 + \exp^{((771.5-X)/61.9)})$, AIC = 48; Satin II: $y = 39.1/(1 + \exp^{((770.8-X)/50.7)})$, AIC = 37; Onyx-AU: $y = 81.6/(1 + \exp^{((839.1-X)/68.7)})$, AIC = 116. (*d*) FLD Expt Pod number – Berken: $y = 33.1/(1 + \exp^{((752.6-X)/48.3)})$, AIC = 84; Jade-AU: $y = 23.4/(1 + \exp^{((768.4-X)/77.6)})$, AIC = 65; Celera II-AU: $y = 42.8/(1 + \exp^{((754.0-X)/47.1)})$, AIC = 87; Opal-AU: $y = 24.5/(1 + \exp^{((788.6-X)/68.1)})$, AIC = 40; Satin II: $y = 34.5/(1 + \exp^{((785.3-X)/48.7)})$, AIC = 45; Onyx-AU: $y = 71.2/(1 + \exp^{((851.0-X)/72.2)})$, AIC = 117.

simple mungbean crop model to identify opportunities for planting in the spring season in the dryland grain production systems of north-eastern Australia. There are substantial opportunities to further improve crop models, crop improvement and agronomic management by quantifying the key determinants of canopy development and reproductive dynamics underpinning yield in mungbean. This has been demonstrated successfully in grain sorghum, where quantification of physiological parameters (Hammer *et al.* 1993; Kim *et al.* 2010*a*, 2010*b*; van Oosterom *et al.* 2011) have led to a robust crop model, integration with plant breeding and improved yield and stability in target production environments (Hammer *et al.* 2010). Critically, the general concepts of crop modelling and simulation for crop adaptation can be used to design crop attributes for future climates (Hammer *et al.* 2020). These concepts can

Table 5. Mean flower appearance rate (FAR) and pod addition rate (PAR) for mungbean genotypes and black gram Onyx-AU.

Experiment	Genotype	FAR (flower (degree-day)$^{-1}$)	PAR (pod (degree-day)$^{-1}$)
Glasshouse (GH)	Berken	0.0187b	0.0198a
	Celera II-AU	0.0175b	0.0176a
	Jade-AU	0.0095a	0.0120ab
	M10403	0.0152b	0.0148a
	Onyx-AU	0.0140b	0.0147a
	Opal-AU	0.0138b	0.0160a
	Satin II	0.0139b	0.0151a
Field (FLD)	Berken	0.0206a	0.0207a
	Celera II-AU	0.0203a	0.0212a
	Jade-AU	0.0132a	0.0129a
	Onyx-AU	0.0146a	0.0139a
	Opal-AU	0.0162a	0.0147a
	Satin II	0.0197a	0.0205a

Each data point is an average across three and four replications in glasshouse (GH) and field (FLD) experiment, respectively. Letters denote significance between genotypes at $P < 0.05$.

be used to design mungbean genotypes or identify traits or practises to improve the crop adaptation to future drier, hotter climates of northern NSW and southern Qld.

In this study, key determinants of canopy development and reproductive dynamics have been quantified in a manner readily usable in mungbean crop model development to support detailed adaptation analysis of trait and management choices on productivity.

Canopy development

Total plant leaf area (TPLA) was related to branching and leaf size

TPLA integrates the number of fully expanded leaves and their leaf area and as such provides an indication of canopy development over time (Hammer *et al.* 2010). In this study, $TPLA_{max}$ was positively associated with TNN, and the residuals of this relationship were positively correlated to average leaf size (R^2 = 0.68, data not shown). The dynamics of $TPLA_{max}$ can be explained by variation in TNN and average leaf size as $TPLA_{max}$ was positively correlated (R^2 = 0.98, data not shown) with the product of TNN × leaf size. For instance, genotypes with a larger main stem leaf area (Opal-AU, Berken and Jade-AU) branched less resulting in greater main stem leaf area early in the season whereas genotypes with smaller main stem leaf area (M10403, Onyx-AU) compensated by producing more secondary and tertiary branches, resulting in greater TPLA. Similar relationships were previously reported in other crops, such as peanut (Halilou *et al.* 2016) and sorghum (Kim *et al.* 2010*a*, 2010*b*), where variations in average leaf size, MSNN and TNN explained the dynamics of TPLA.

The bi-linear model adequately quantified the relationship between TNN and MSNN for mungbean in the present study. The number of total nodes produced per node on the main stem for *Phase I* was 1.05, similar to values in *Phase I* reported for chickpea (Robertson *et al.* 2002). Another study on chickpea reported a key difference, with three nodes produced for each node on main stem in *Phase I*, accounting for more branches (Soltani *et al.* 2006). Increases in TNN in *Phase II* were related to the appearance of primary and secondary branches in mungbean, similar to chickpea (Soltani *et al.* 2006). The bi-linear model further confirmed that variation in TNN was a result of genotypic variation in MSNN during *Phase II* in mungbean, indicating that some genotypes (Celera II-AU, Jade-AU and Satin II) depleted the available nodes on the main stem to branch. TNN has been identified as an important trait for simulating plant leaf area (Sinclair 1984) and predictions of TNN are possible from MSNN. While, dissecting determinants of canopy development will likely continue in future, studies should target increases in MSNN to increase TNN, without compromising leaf size and TPLA if possible.

A simple, robust, and general framework predicted leaf area by incorporating the impact of different leaf sizes at each node and TNN. The parameters TNN and leaf size both provide avenues for genotypic control of leaf area production and thus, are required to use this framework. While this paper presents the framework for TPLA prediction using known values for TNN, TNN can be predicted from MSNN following the bi-linear equation given in Fig. 2 and thus, information on branching pattern and architecture is crucial to apply this predictive framework in mungbean.

Thermal time drives canopy development

Similar to crops such as peanut (Halilou *et al.* 2016) and chickpea (Soltani *et al.* 2006), canopy development in mungbean was closely associated with thermal time (Chauhan and Williams 2018). Thermal time underpinned the development of the canopy through effects on LAR and TNN. Given TNN and leaf size, $TPLA_{max}$ can be accurately predicted from thermal time. Precise determination of thermal time is thus critical for prediction of canopy development.

In this study, temperature variation between the two environments, particularly large diurnal temperature variation in the FLD Expt, resulted in differences observed in thermal time calculations (Fig. 1). Cardinal temperatures are also likely to play a role in inaccuracies in thermal time calculations. At present, a T_b of 7.5°C is applied in calculations of thermal time to flowering in mungbean (Ellis *et al.* 1994). The method used by Ellis *et al.* (1994) to derive T_b may have limitations as using average temperatures over developmental periods can introduce significant bias in comparison to more recent optimisation methods

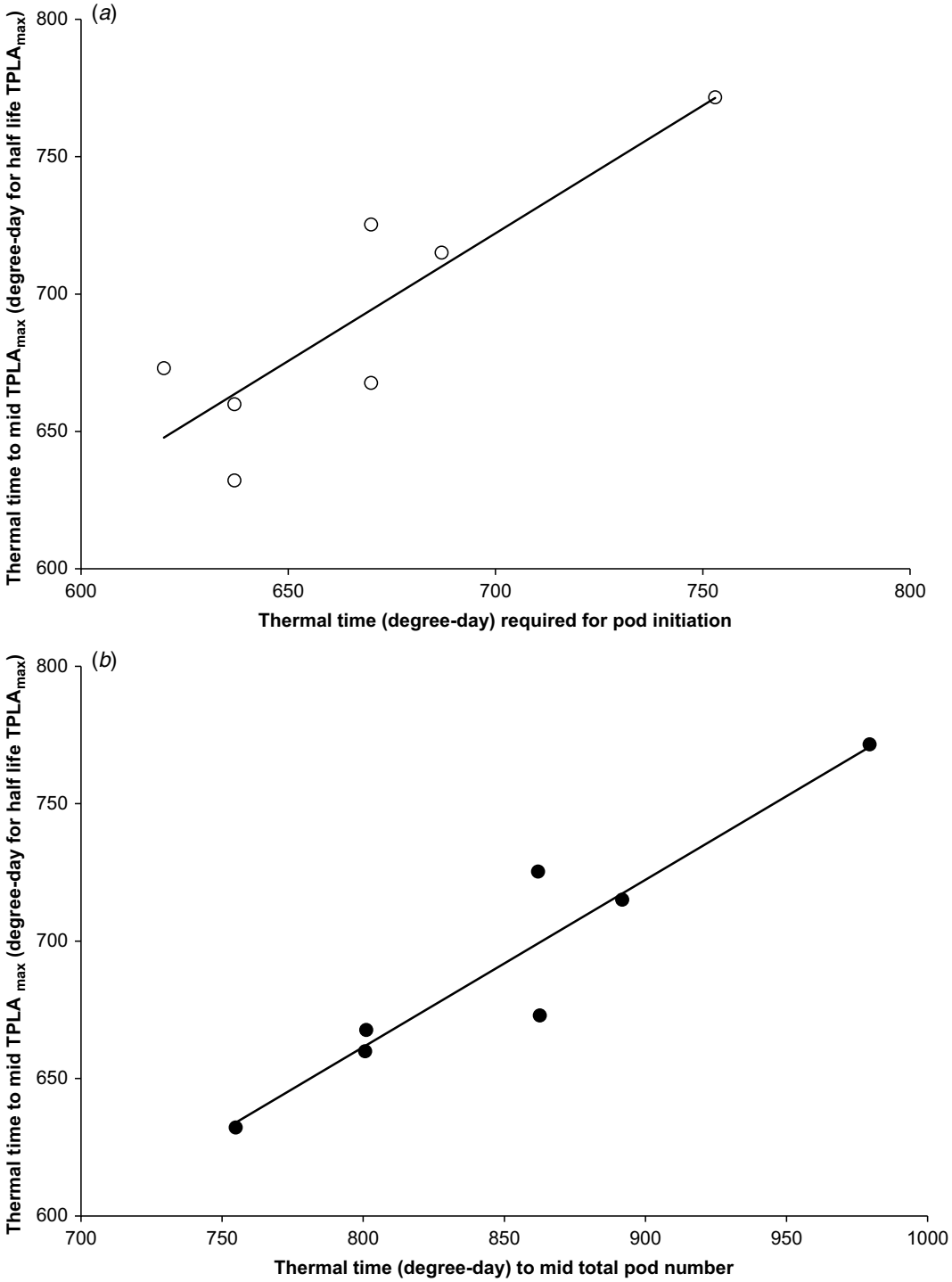

Fig. 6. (*a*) Relationship between thermal time to reach half of $TPLA_{max}$ (*a*) and thermal time required for pod initiation (TTPI) (degree-day) across all mungbean genotypes and Onyx-AU in the glasshouse experiment (GH Expt). Regression: $a = 0.93 \times TTPI + 71.6$, $R^2 = 0.75$, $P = 0.01$, $n = 7$. (*b*) Relationship between thermal time to reach half of $TPLA_{max}$ (*a*) and thermal time to reach mid total pod number (TTPN) (degree-day) for all mungbean genotypes and Onyx-AU in the glasshouse experiment (GH Expt). Regression is $a = 0.61 \times TTPN + 174.8$, $R^2 = 0.89$, $P = 0.0012$, $n = 7$.

when fitting daily rate of development models (e.g. Ravi Kumar *et al.* 2009). Similarly, the occurrence of supra-optimal temperatures in the FLD Expt, may have contributed to differences in thermal time calculations as

the responses of phenology to such high temperatures have not been quantified well (Wang *et al.* 2017).

Additionally, T_b would have been underestimated if the optimum temperature estimates were influenced by photoperiod (Ellis *et al.* 1994). Photoperiodism regulates flowering in some crops, and earlier mungbean genotypes are known to be affected by photo-thermal interactions on time to flower (Swindell and Poehlman 1978; Ellis *et al.* 1994; Rebetzke and Lawn 2006). Despite this, the current APSIM mungbean model notes that the phenology of mungbean cultivars are photoperiod insensitive and uses thermal time to drive phenological development. It is not clear if the genotypes currently produced in Australia, many of which are included in this study, are photoperiod insensitive. To overcome inconsistencies in thermal time, further research on photoperiod and cardinal temperatures is required for current commercial mungbean cultivars.

Reproductive dynamics

Timing of initiation and rate of flowering related to thermal time

The timing and initiation of flowering in mungbean is related to thermal time (Chauhan and Williams 2018). Genotypic variability was observed for time to first and 50% flowering (Table 5) in the present study, as previously reported in other mungbean genotypes (Lawn 1979; Ellis *et al.* 1994; Khattak *et al.* 2002; Rebetzke and Lawn 2006). In this study, Celera II-AU produced higher numbers of flowers and pods early in the season compared to other genotypes, similar to results for mungbean in Bangladesh (Mondal *et al.* 2011). Variation in time to 50% flowering influenced flowering duration among the genotypes (Fig. 6). The FLD Expt and GH Expt showed similar rankings for rates of flowering and podding as well as flowering duration but differed in magnitude. These differences may be a result of differences in temperature–radiation balance and possibly variable and higher temperatures in the FLD Expt during flowering and podding (36–55 DAS) (Fig. 1), which further highlights the potential inaccuracies in cardinal temperatures, particularly, optimum and maximum temperatures for mungbean. Future studies should focus on cardinal temperature assessment using thermal plate, and rate of development to flowering using different temperature regimes in temperature-controlled glasshouse experiments for the current mungbean genotypes.

Timing of active pod development associated with near cessation of leaf area development

Interactions of reproductive growth with canopy development was likely a consequence of source–sink dynamics, driven by internal plant competition for assimilates (Luquet *et al.* 2006; Alam *et al.* 2014). Mature leaves are typically a net source of assimilate whereas sinks (roots, flowers, pods, expanding leaves) are net-importers of assimilates (Ludewig and Flügge 2013). Hence, the timing of flowering and pod development in relation to canopy development is critical to yield formation. Phenology plays a critical role in source–sink dynamics as the slowing of canopy development occurred when demand for photoassimilate by reproductive sinks reached a critical threshold. This study demonstrated that the mid-podding stage, when pods transition into dominant sinks, was associated with the near cessation of increase in TPLA (Fig. 6*b*). It is plausible that this is driven by internal plant competition for assimilates between flowers, developing pods and alternative sinks (leaves, stem, roots) as was found in sorghum (Kim *et al.* 2010*a*, 2010*b*; Alam *et al.* 2014).

In legumes, flowers and pods produced later in the crop cycle are highly likely to abscise when assimilate demand cannot be met (Bruening and Egli 1999; Egli and Bruening 2002*a*, 2002*b*; Smith *et al.* 2019). Mungbean yield is known to be limited by the premature abscission of flowers and pods (Clifford 1979). While the present study did not consider pod abscission in calculation of pod set, it is likely that pod abscission that occurred at later stages of the podding phase was influenced by increased sink demands. Previous research demonstrated that removal of mungbean pods resulted in increased biomass of alternative sinks, such as leaves and stems (Mitra and Ghildiyal 1988). This suggests that limited assimilate supply can abscise young, developing pods and seeds, as was found in chickpea (Pang *et al.* 2017).

The cessation of canopy development in mungbean through the inhibition of additional node production, likely occurred in response to alterations in source–sink dynamics triggered through pod development. To enhance reproduction in mungbean, it is imperative to balance the assimilate supply from canopy development with the sink demand by the developing pods, which requires the establishment of a large canopy at flowering and cessation of further canopy growth at mid podding stage.

Conclusion

This study underpins the development of a quantitative framework for physiological determinants of canopy and reproductive development in current commercial Australian mungbean genotypes. It provides an important link between canopy development and its interaction with flower and pod addition dynamics. Mungbean genotypes varied in their LAR on the main stem, which determined the final and total number of nodes and leaf area on the plant, ensuring adequate TPLA through the reproductive phase. Throughout the life cycle of mungbean, traits determining canopy and reproductive development, operating at different stages

could be explained on the basis of responses to temperature and source–sink interactions *via* internal plant competition. Hence, this study provides a quantitative basis to evaluate the effects of temperature and source-sink dynamics in response to growing environments, through the use of this improved understanding and quantification of canopy development and reproductive dynamics to enhance existing modelling capability.

Supplementary material

Supplementary material is available online.

References

Akpapunam M (1996) Mung bean (Vigna radiata (L.) Wilczek). In 'Food and Feed from Legumes and Oilseeds.' (Eds E Nwokolo, J Smartt) pp. 209–215. (Springer: Boston, MA, USA)

Alam MM, Hammer GL, Oosterom EJ, Cruickshank AW, Hunt CH, Jordan DR (2014) A physiological framework to explain genetic and environmental regulation of tillering in sorghum. *New Phytologist* **203**, 155–167. doi:10.1111/nph.12767

Australian Bureau of Metrology (2021) Past weather data: temperature, rainfall and solar radiation. Available at http://www.bom.gov.au

Bruening WP, Egli DB (1999) Relationship between photosynthesis and seed number at phloem isolated nodes in soybean. *Crop Science* **39**, 1769–1775. doi:10.2135/cropsci1999.3961769x

Chauhan YS, Rachaputi RCN (2014) Defining agro-ecological regions for field crops in variable target production environments: a case study on mungbean in the northern grains region of Australia. *Agricultural and Forest Meteorology* **194**, 207–217. doi:10.1016/j.agrformet.2014.04.007

Chauhan Y, Williams R (2018) Physiological and agronomic strategies to increase mungbean yield in climatically variable environments of Northern Australia. *Agronomy* **8**, 83. doi:10.3390/agronomy8060083

Clifford PE (1979) Source limitation of sink yield in mung beans. *Annals of Botany* **43**, 397–399. doi:10.1093/oxfordjournals.aob.a085648

Cohen D (1976) The optimal timing of reproduction. *The American Naturalist* **110**, 801–807. doi:10.1086/283103

Egli DB, Bruening WP (2002*a*) Flowering and fruit set dynamics at phloem-isolated nodes in soybean. *Field Crops Research* **79**, 9–19. doi:10.1016/S0378-4290(02)00016-3

Egli DB, Bruening WP (2002*b*) Synchronous flowering and fruit set at phloem-isolated nodes in soybean. Crop Science 42, 1535–1540. https://doi.org/10.2135/cropsci2002.1535

Ellis RH, Lawn RJ, Summerfield RJ, Qi A, Roberts EH, Chay PM, Brouwer JB, Rose JL, Yeates SJ, Sandover S (1994) Towards the reliable prediction of time to flowering in six annual crops. IV. Cultivated and wild mung bean. *Experimental Agriculture* **30**, 31–43. doi:10.1017/S0014479700023826

Halilou O, Hissene HM, Clavijo Michelangeli JA, Hamidou F, Sinclair TR, Soltani A, Mahamane S, Vadez V (2016) Determination of coefficient defining leaf area development in different genotypes, plant types and planting densities in peanut (*Arachis hypogeae* L.). *Field Crops Research* **199**, 42–51. doi:10.1016/j.fcr.2016.09.013

Hammer GL, Carberry PS, Muchow RC (1993) Modelling genotypic and environmental control of leaf area dynamics in grain sorghum. I. Whole plant level. *Field Crops Research* **33**, 293–310. doi:10.1016/0378-4290(93)90087-4

Hammer GL, van Oosterom E, McLean G, Chapman SC, Broad I, Harland P, Muchow RC (2010) Adapting APSIM to model the physiology and genetics of complex adaptive traits in field crops. *Journal of Experimental Botany* **61**, 2185–2202. doi:10.1093/jxb/erq095

Hammer GL, McLean G, Oosterom E, Chapman S, Zheng B, Wu A, Doherty A, Jordan D (2020) Designing crops for adaptation to the drought and high-temperature risks anticipated in future climates. *Crop Science* **60**, 605–621. doi:10.1002/csc2.20110

Imrie BC, Lawn RJ (1990) Time to flowering of mung bean (*Vigna radiata*) genotypes and their hybrids in response to photoperiod and temperature. *Experimental Agriculture* **26**, 307–318. doi:10.1017/S0014479700018470

Jones CA, Kiniry JR (1986) 'CERES-maize: a simulation model of maize growth and development.' (Texas A&M: College Station, USA)

Kaur R, Bains TS, Bindumadhava H, Nayyar H (2015) Responses of mungbean (*Vigna radiata* L.) genotypes to heat stress: effects on reproductive biology, leaf function and yield traits. *Scientia Horticulturae* **197**, 527–541. doi:10.1016/j.scienta.2015.10.015

Khattak GSS, Haq MA, Ashraf M, Hassan S (2002) Yield and yield components at various flower flushes in mungbean (*Vigna radiata* (L.) Wilczek). *Breeding Science* **52**, 61–63. doi:10.1270/jsbbs.52.61

Kim HK, Luquet D, van Oosterom E, Dingkuhn M, Hammer G (2010*a*) Regulation of tillering in sorghum: genotypic effects. *Annals of Botany* **106**, 69–78. doi:10.1093/aob/mcq080

Kim HK, van Oosterom E, Dingkuhn M, Luquet D, Hammer G (2010*b*) Regulation of tillering in sorghum: environmental effects. *Annals of Botany* **106**, 57–67. doi:10.1093/aob/mcq079

Lawn RJ (1979) Agronomic studies on *Vigna* spp. in south-eastern Queensland. I. Phenological response of cultivars to sowing date. *Australian Journal of Agricultural Research* **30**, 855–870. doi:10.1071/AR9790855

Lenth RV (2021) emmeans: estimated marginal means aka least-squares means. R package version 1.4.2. Available at https://CRAN.R-project.org/package=emmeans

Littleton EJ, Dennett MD, Elston J, Monteith JL (1979) The growth and development of cowpeas (*Vigna unguiculata*) under tropical field conditions: 1. Leaf area. *The Journal of Agricultural Science* **93**, 291–307. doi:10.1017/S0021859600037977

Ludewig F, Flügge U-I (2013) Role of metabolite transporters in source-sink carbon allocation. *Frontiers in Plant Science* **4**, 231. doi:10.3389/fpls.2013.00231

Luquet D, Dingkuhn M, Kim H, Tambour L, Clement-Vidal A (2006) *EcoMeristem*, a model of morphogenesis and competition among sinks in rice. 1. Concept, validation and sensitivity analysis. *Functional Plant Biology* **33**, 309–323. doi:10.1071/FP05266

Mitra S, Ghildiyal MC (1988) Photosynthesis and assimilate partitioning in mungbean in response to source-sink alteration. *Journal of Agronomy and Crop Science* **160**, 303–308. doi:10.1111/j.1439-037X.1988.tb00626.x

Mondal MMA, Fakir M, Juraimi A, Hakim M, Ismal M, Shamsuddoha A (2011) Effects of flowering behavior and pod maturity synchrony on yield of mungbean [*Vigna radiata* (L.) Wilczek]. *Australian Journal of Crop Science* **5**, 945–953.

Morrison MJ, McVetty PBE (1991) Leaf appearance rate of summer rape. *Canadian Journal of Plant Science* **71**, 405–412. doi:10.4141/cjps91-056

Muchow RC (1985) Phenology, seed yield and water use of grain legumes grown under different soil water regimes in a semi-arid tropical environment. *Field Crops Research* **11**, 81–97. doi:10.1016/0378-4290(85)90093-0

Muchow RC, Robertson MJ, Pengelly BC (1993) Accumulation and partitioning of biomass and nitrogen by soybean, mungbean and cowpea under contrasting environmental conditions. *Field Crops Research* **33**, 13–36. doi:10.1016/0378-4290(93)90092-2

Mwanamwenge J, Siddique KHM, Sedgley RH (1997) Canopy development and light absorption of grain legume species in a short season Mediterranean-type environment. *Journal of Agronomy and Crop Science* **179**, 1–7. doi:10.1111/j.1439-037X.1997.tb01141.x

Nair RM, Yang R-Y, Easdown WJ, Thavarajah D, Thavarajah P, Hughes Jd'A, Keatinge JDH (Dyno) (2013) Biofortification of mungbean (*Vigna radiata*) as a whole food to enhance human health. *Journal of the Science of Food and Agriculture* **93**, 1805–1813. doi:10.1002/jsfa.6110

Nair RM, Schafleitner R, Easdown W, Ebert A, Hanson P, Hughes Jd'A, Keatinge JDH (2014) Legume improvement program at AVRDC – the world vegetable center: impact and future prospects. *Ratarstvo i Povrtarstvo* **51**, 55–61. doi:10.5937/ratpov51-5488

Nelder J (2017) 'Genstat.' (VSN International: UK)

Overman AR, Scholtz III RV (2002) Growth response models. In 'Mathematical models of crop growth and yield'. (Ed. M Dekker) pp. 1–12. (Marcel Dekker: New York, NY, USA)

Pang J, Turner NC, Khan T, Du Y-L, Xiong J-L, Colmer TD, Devilla R, Stefanova K, Siddique KHM (2017) Response of chickpea (*Cicer arietinum* L.) to terminal drought: leaf stomatal conductance, pod abscisic acid concentration, and seed set. *Journal of Experimental Botany* **68**, 1973–1985. doi:10.1093/jxb/erw153

Pengelly BC, Muchow RC, Blamey FPC (1999) Predicting leaf area development in response to temperature in three tropical annual forage legumes. *Australian Journal of Agricultural Research* **50**, 253–259. doi:10.1071/A98055

Pinheiro JC, Bates DM, DebRoy S, Sarkar D (2021) 'nlme: linear and nonlinear mixed effects models.' (Springer: New York, NY, USA)

Profillidis VA, Botzoris GN (2019) Chapter 6 - Trend projection and time series methods. In 'Modeling of transport demand: analyzing, calculating, and forecasting transport demand'. (Eds VA Profillidis, GN Botzoris) pp. 225–270. (Elsevier: Netherlands)

Queensland Government (2016) Common soil types. Available at https://www.qld.gov.au/environment/land/management/soil/soil-testing/types

R Core Team (2021) 'R: a language and environment for statistical computing.' (R Foundation for Statistical Computing: Vienna, Austria)

Rachaputi RCN, Chauhan Y, Douglas C, Martin W, Krosch S, Agius P, King K (2015) Physiological basis of yield variation in response to row spacing and plant density of mungbean grown in subtropical environments. *Field Crops Research* **183**, 14–22. doi:10.1016/j.fcr.2015.07.013

Rachaputi RCN, Sands D, McKenzie K, Agius P, Lehane J, Seyoum S (2019) Eco-physiological drivers influencing mungbean [*Vigna radiata* (L.) Wilczek] productivity in subtropical Australia. *Field Crops Research* **238**, 74–81. doi:10.1016/j.fcr.2019.04.023

Ranganathan R, Chauhan YS, Flower DJ, Robertson MJ, Sanetra C, Silim SN (2001) Predicting growth and development of pigeonpea: leaf area development. *Field Crops Research* **69**, 163–172. doi:10.1016/S0378-4290(00)00137-4

Ravi Kumar S, Hammer GL, Broad I, Harland P, McLean G (2009) Modelling environmental effects on phenology and canopy development of diverse sorghum genotypes. *Field Crops Research* **111**, 157–165. doi:10.1016/j.fcr.2008.11.010

Rebetzke GJ, Lawn RJ (2006) Adaptive responses of wild mungbean (*Vigna radiata* ssp. sublobata) to photo-thermal environment. I. Phenology. *Australian Journal of Agricultural Research* **57**, 917–928. doi:10.1071/AR05357

Robertson MJ, Carberry PS, Lucy M (2000) Evaluation of a new cropping option using a participatory approach with on-farm monitoring and simulation: a case study of spring-sown mungbeans. *Australian Journal of Agricultural Research* **51**, 1–12. doi:10.1071/AR99082

Robertson MJ, Carberry PS, Huth NI, Turpin JE, Probert ME, Poulton PL, Bell M, Wright GC, Yeates SJ, Brinsmead RB (2002) Simulation of growth and development of diverse legume species in APSIM. *Australian Journal of Agricultural Research* **53**, 429–446. doi:10.1071/AR01106

Robertson MJ, Rebetzke GJ, Norton RM (2015) Assessing the place and role of crop simulation modelling in Australia. *Crop & Pasture Science* **66**, 877–893. doi:10.1071/CP14361

Sharma L, Priya M, Bindumadhava H, Nair RM, Nayyar H (2016) Influence of high temperature stress on growth, phenology and yield performance of mungbean [*Vigna radiata* (L.) Wilczek] under managed growth conditions. *Scientia Horticulturae* **213**, 379–391. doi:10.1016/j.scienta.2016.10.033

Sinclair TR (1984) Leaf area development in field-grown soybeans. *Agronomy Journal* **76**, 141–146. doi:10.2134/agronj1984.00021962007600010034x

Smith MR, Veneklaas E, Polania J, Rao IM, Beebe SE, Merchant A (2019) Field drought conditions impact yield but not nutritional quality of the seed in common bean (*Phaseolus vulgaris* L.). *PLoS ONE* **14**, 1–18. doi:10.1371/journal.pone.0217099

Soltani A, Robertson MJ, Mohammad-Nejad Y, Rahemi-Karizaki A (2006) Modeling chickpea growth and development: leaf production and senescence. *Field Crops Research* **99**, 14–23. doi:10.1016/j.fcr.2006.02.005

Swindell RE, Poehlman JM (1978) Inheritance of photoperiod response in mungbean (*Vigna radiata* [L.] Wilczek). *Euphytica* **27**, 325–333. doi:10.1007/BF00039150

Thomas, Robertson MJ, Fukai S, Peoples MB (2004) The effect of timing and severity of water deficit on growth, development, yield accumulation and nitrogen fixation of mungbean. *Field Crops Research* **86**, 67–80. doi:10.1016/S0378-4290(03)00120-5

van Oosterom EJ, Borrell AK, Deifel KS, Hammer GL (2011) Does increased leaf appearance rate enhance adaptation to postanthesis drought stress in sorghum? *Crop Science* **51**, 2728–2740. doi:10.2135/cropsci2011.01.0031

Wang E, Martre P, Zhao Z, Ewert F, Maiorano A, Rötter RP, Kimball BA, Ottman MJ, Wall GW, White JW, Reynolds MP, Alderman PD, Aggarwal PK, Anothai J, Basso B, Biernath C, Cammarano D, Challinor AJ, De Sanctis G, Doltra J, Dumont B, Fereres E, Garcia-Vila M, Gayler S, Hoogenboom G, Hunt LA, Izaurralde RC, Jabloun M, Jones CD, Kersebaum KC, Koehler A-K, Liu L, Müller C, Kumar SN, Nendel C, O'Leary G, Olesen JE, Palosuo T, Priesack E, Rezaei EE, Ripoche D, Ruane AC, Semenov MA, Shcherbak I, Stöckle C, Stratonovitch P, Streck T, Supit I, Tao F, Thorburn P, Waha K, Wallach D, Wang Z, Wolf J, Zhu Y, Asseng S (2017) The uncertainty of crop yield projections is reduced by improved temperature response functions. *Nature Plants* **3**, 17102. doi:10.1038/nplants.2017.102

Data availability. The data that support this study will be shared upon reasonable request to the corresponding author.

Conflicts of interest. The authors declare no conflicts of interest.

Declaration of funding. The authors acknowledge the Grains Research and Development Corporation (GRDC) for funding the Optimising mungbean yield (Grant number-GRDC 9176395) – mungbean physiology project (UOQ1808-003RTX) through which these experiments were conducted.

Acknowledgements. The authors thank the National Mungbean Improvement Program (Qld DAF) for the germplasm used in this study. The late maturity, high biomass breeding line M10403 was developed by the Grains Research and Development Corporation and DAF National Mungbean Improvement Program. The help of Mr. T. Rossignol and Dr. K. Wenham in providing support and advice in conducting these experiments is gratefully acknowledged. Geetika Geetika was supported by a UQ Research Training Scholarship.

Author affiliations

[A]Queensland Alliance for Agriculture and Food Innovation, The University of Queensland, Gatton, Qld 4343, Australia.

[B]Animal, Plant and Soil Sciences, La Trobe University, Melbourne, Vic. 3086, Australia.

[C]Queensland Alliance for Agriculture and Food Innovation, The University of Queensland, St Lucia, Qld 4067, Australia.

[D]School of Agriculture and Food Sciences, The University of Queensland, Gatton, Qld 4343, Australia.